

## Closure of plasmodesmata in maize (*Zea mays*) at low temperature: a new mechanism for inhibition of photosynthesis

Anna Bilska<sup>1</sup> and Paweł Sowiński<sup>1,2,\*</sup>

<sup>1</sup>Department of Plant Biochemistry and Physiology, Plant Breeding and Acclimatization Institute, Radzików, 05-870 Błonie, Poland and <sup>2</sup>Department of Plant Molecular Ecophysiology, Institute of Plant Experimental Biology, Faculty of Biology, University of Warsaw, Miecznikowa 1, 02-096 Warszawa, Poland

\* For correspondence. E-mail pawes@biol.uw.edu.pl

Received: 7 April 2010 Returned for revision: 26 June 2010 Accepted: 12 July 2010 Published electronically: 29 September 2010

• **Background and Aims** Photosynthesis is one of the processes most susceptible to low-temperature inhibition in maize, a tropical C4 crop not yet fully adapted to a temperate climate. C4 photosynthesis relies on symplasmic exchange of large amounts of photosynthetic intermediates between Kranz mesophyll (KMS) and bundle sheath (BS) cells. The aim of this study was to test the hypothesis that the slowing of maize photosynthesis at low temperature is related to ultrastructural changes in the plasmodesmata between KM and BS as well as BS and vascular parenchyma (VP) cells.

• **Methods** Chilling-tolerant (CT) KW 1074 and chilling-sensitive (CS) CM 109 maize (*Zea mays*) lines were studied. The effect of moderate chilling (14 °C) on the rate of photosynthesis, photosynthate transport kinetics, and the ultrastructure of plasmodesmata linking the KMS, BS and VP cells were analysed. Additionally, the accumulation of callose and calreticulin was studied by the immunogold method.

• **Key Results** Chilling inhibited photosynthesis, photosynthate transfer to the phloem and photosynthate export from leaves in both lines. This inhibition was reversible upon cessation of chilling in the CT line but irreversible in the CS line. Simultaneously to physiological changes, chilling induced swelling of the sphincters of plasmodesmata linking KMS and BS cells and a decreased lumen of the cytoplasmic sleeve of plasmodesmata at the BS/VP interface in the CS line but not in the CT line. Accumulation of calreticulin, which occurred near the neck region of the closed plasmodesmata was observed after just 4 h of chilling and over-accumulation of callose at the KMS/BS and BS/VP interfaces occurred after 28 h of chilling.

• **Conclusions** Stronger chilling sensitivity of the CM 109 maize line compared with the KW 1074 line, shown by decreased photosynthesis and assimilate export from a leaf, is related to changes in the ultrastructure of leaf plasmodesmata at low temperature. The chain of reactions to chilling is likely to include calreticulin action resulting in rapid and efficient closure of the plasmodesmata at both KMS/BS and BS/VP interfaces. Callose deposition in a leaf was a secondary effect of chilling.

**Key words:** Callose, calreticulin, chilling, electron tomography, phloem loading, photosynthesis inhibition, plasmodesmata ultrastructure, symplasmic transport, *Zea mays*.

### INTRODUCTION

Photosynthesis is one of the processes most susceptible to low-temperature inhibition in maize (*Zea mays*), a tropical C4 crop not yet fully adapted to temperate climates (Greaves, 1996; Foyer *et al.*, 2002). Among the many aspects of photosynthesis likely to be inhibited by sub-optimal temperatures, the importance of short-distance transport of photosynthetic intermediates between cells and phloem loading has not been adequately evaluated, and has probably been underestimated. C4 photosynthesis requires symplasmic exchange of large quantities of photosynthetic intermediates between the chlorenchymatous Kranz mesophyll cells (KMS) and bundle sheath (BS) cells (Fig. 1).

In maize, as in other C4 plants, short-distance transport of photosynthates is through numerous plasmodesmata which cross the suberin lamella; this is impermeable to aqueous solutions (Evert *et al.*, 1996, but see Eastman *et al.*, 1988a, b).

Sucrose, the end-product of photosynthetic carbon metabolism, before being loaded into sieve elements, also moves symplasmically from the site of synthesis, the KMS cells (Furbank *et al.*, 1985; Provencher *et al.*, 2001), through BS cells to the vascular parenchyma (VP) cells. Phloem loading of sucrose is achieved by an apoplasmic mechanism (Thompson *et al.*, 1979, but see Sowiński *et al.*, 2003) with the participation of the sucrose transporter ZmSUT1 (Aoki *et al.*, 1999). According to Fritz *et al.* (1983), sucrose is loaded by thin-walled sieve tubes, without the participation of companion cells.

Long (1983) postulated that low temperature slows the transfer of carbon between the C4 and the C3 pathway. Later it was found that the time needed for <sup>14</sup>C-assimilate to be transferred to the transport path was much greater at low temperature in a chilling-sensitive inbred line of maize than in chilling-tolerant one (Sowiński *et al.*, 2003). We hypothesize that this is an effect of closure of plasmodesmata between the different cell types (KMS, BS and VP). Gamalei *et al.* (1994) suggested that low

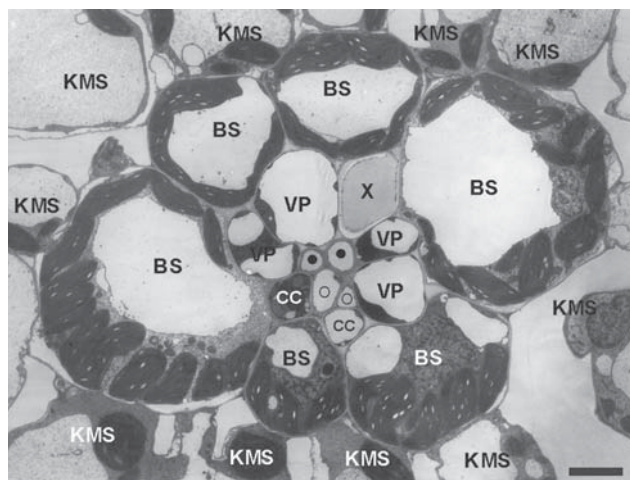


FIG. 1. Cross-section of small bundle in a juvenile maize leaf. KMS, Kranz mesophyll; BS, bundle sheath; VP, vascular parenchyma; CC, companion cell; O, thin-walled sieve tube; •, thick-walled sieve tube; X, xylem. Scale bar = 5  $\mu\text{m}$ .

temperature (10 °C) caused drastic changes in the endoplasmic reticulum (ER) and contraction of the desmotubule, assumed by these authors to be the transport compartment of plasmodesmata. This was observed in intermediary cells, the specialized companion cells in symplasmic phloem loaders. Very rapid restriction of symplasmic communication in the cold was postulated by Holdaway-Clarke *et al.* (2000). However, they did not study the ultrastructure of plasmodesmata.

Limitation, by chilling, of short-distance transport of C4 intermediates between KMS and BS would have important consequences for the chilling-sensitivity of maize. Low temperature limits the sinks for the absorbed excitation energy and excessive electrons react with oxygen, thus leading to production of reactive oxygen species. In maize, some antioxidants are differentially distributed between KMS and BS cells (Doullis *et al.*, 1997) and some intermediates necessary for the recycling of antioxidants must be transported between the cells. Therefore, it is reasonable to hypothesize that chilling-induced photoinhibition in maize leaves results from inhibition of short-distance transport in leaf and decreased export of photosynthate at low temperature.

The aim of this study was to test the hypothesis that reduced photosynthesis of maize at low temperature is related to ultrastructural changes in plasmodesmata between the KMS and BS, and BS and VP cells and/or to the inhibition of photosynthate export from leaves. Thus, both  $^{14}\text{C}$ -assimilate transport kinetics and ultrastructure of plasmodesmata at KMS/BS and BS/VP interfaces has been studied in chilling-tolerant and chilling-sensitive inbred maize lines after different periods of chilling. Small and intermediate bundle sheaths (Fritz *et al.*, 1983) were chosen because they are involved in assimilate loading (Evert *et al.*, 1996). Additionally, the accumulation of callose, a polysaccharide responsible for closure of plasmodesmata in maize leaves (Botha *et al.*, 2000), and calreticulin, a calcium-sequestering protein involved in the control of the plasmodesmata size exclusion limit (Baluška *et al.*, 1999; Blackmann *et al.*, 1999), was studied.

## MATERIALS AND METHODS

### *Plant material, growth conditions and chilling treatment*

Chilling-tolerant (CT) KW 1074 (*Zea mays* spp. *indurata*, flint) and chilling-sensitive (CS) CM 109 maize (*Z. mays* spp. *indentata*, dent) lines were analysed; their characteristics have been described in other papers (Verheul *et al.*, 1996; Janda *et al.* 1998).

Kernels were germinated for 3 d in wet sand in darkness at 24 °C. Then, plants were transferred to pots containing Knop's nutrient solution, supplemented with Hoagland's micro-nutrients, and were grown in a growth chamber with 14 h light/10 h darkness, irradiance 250  $\mu\text{mol quanta m}^{-2} \text{s}^{-1}$  at 24 °C /22 °C day/night temperature. When the 3rd leaf was fully developed, at the beginning of the light period, plants were transferred to low temperature 14 °C/12 °C day/night for either 4 or 28 h, except for plants chilled for 1 h, which were transferred to a cold chamber 3 h after illumination.

### *Chlorophyll fluorescence*

Maximal quantum yield of PSII electron transport ( $F_v/F_m$ , ratio of variable to maximal fluorescence) was measured with a fluorometer (PAM 200, H. Walz, Germany) in plants chilled for 4 and 28 h. In control plants,  $F_v/F_m$  was measured 4 h after illumination. Before measurements of  $F_v/F_m$ , plants were dark adapted for 30–60 min at 24 °C. Experiments were repeated three times using three plants per line per experimental variant. Data were statistically analysed ( $P < 0.05$ ) by analysis of variance using STATISTICA PL (StatSoft®).

### *$^{14}\text{C}$ assimilate transport*

Net  $\text{CO}_2$  assimilation rate and transport kinetics were measured in plants: (a) controls – measured both at 24 °C and 14 °C; (b) chilled for 1 and 4 h measured at 24 °C; (c) chilled for 28 h – measured both at 24 °C and 14 °C. Net  $\text{CO}_2$  assimilation rate was determined in a closed-type gas-exchange system using an infrared  $\text{CO}_2$  analyser (AirTECH 2500-P; GAZEX Co., Poland). During the experiments, the PPFD was 400  $\mu\text{mol quanta m}^{-2} \text{s}^{-1}$  and the temperature 24 °C or 14 °C for both control and chilling-treated plants. Each measurement of photosynthesis was replicated three to five times.

In this study, two transport parameters – the time of  $^{14}\text{C}$ -assimilate appearance in the transport path (AT, a measure of photosynthate transfer rate into the phloem-loading zone) and the fraction of incorporated radioactivity exported from the leaf (RL, a measure of phloem loading rate) – were evaluated by an *in vivo* method (Sowiński *et al.*, 2003), which is briefly described. Transport kinetics were estimated by following the movement of radioactivity along a leaf following a short period of assimilation of  $^{14}\text{CO}_2$  ('pulse') (Thompson *et al.*, 1979) using three beryllium window proportional counters, which measure X-ray (Bremsstrahlung) radiation originating from interaction of  $^{14}\text{C}$   $\beta$  particles with leaf tissue, positioned along the leaf blade.

Transport was measured on the third leaf between 3 and 7 h after illumination in the growth chamber. Irradiance during the experiments was 400  $\mu\text{mol quanta m}^{-2} \text{s}^{-1}$ . After minimum of 30 min of adaptation, net  $\text{CO}_2$  assimilation rate was

determined followed by  $^{14}\text{C}$  (1.85 MBq) feeding (approx. 10 min) into a small area in the middle of the leaf; movement of  $^{14}\text{C}$  along the leaf blade was followed until the radioactivity measured by the first detector dropped from its maximum to the minimum (2–3 h). For calculations of transport parameters, radioactivity curves obtained from three detectors were used. AT was estimated as the time necessary for the label to move between the first and the second detector (located 2 cm below the first one) minus the time of label movement between the second and the third detector (located 2 cm below the second one). RL (the fraction of incorporated radioactivity exported from the leaf, in percentage of the maximum) was estimated as the difference between maximum and minimum radioactivity measured at the first detector. Experiments were repeated three times using three to five plants per line per experimental variant. Data were statistically analysed ( $P < 0.05$ ) by analysis of variance using STATISTICA PL (StatSoft®).

#### Structure of plasmodesmata

For ultrastructure studies of plasmodesma, samples were harvested from plants chilled for 1, 4, 12 and 28 h. Control plants were taken 4 h after illumination. Samples taken from the leaf blade region located between the upper one-third and the middle part of an intact, fully developed third leaf were fixed in 2.5 % glutaraldehyde (with or without 0.5 % tannic acid) in 0.1 M phosphate buffer, pH 7.3, for 4 h and post-fixed with 1 % osmium tetroxide for 2 h (both at room temperature). After dehydration (ethanol 10–100 %) the material was embedded in Epon resin and polymerized for 24 h at 60 °C. Ultrathin (80 nm) sections were cut with a diamond knife on a Leica Ultracut UTC ultramicrotome and stained with uranyl acetate and lead citrate. Sections were examined under a transmission electron microscope (model JEM-1200EX; JEOL Co., Japan). Electron microscope observations were done in the Laboratory of Electron Microscopy, Nencki Institute of Experimental Biology (Warsaw, Poland).

Cell interfaces were photographed at  $\times 60\,000$  primary magnification and the ultrastructure of plasmodesmata was evaluated from the photographs. Chilling-induced enlargement of electron-dense elements in neck regions of KMS/BS plasmodesmata, here called sphincters after Evert *et al.* (1977), was estimated visually and was presented as the percentage of plasmodesmata showing clear-cut swelling of the sphincter among all the plasmodesmata analysed. The lumen of the cytoplasmic sleeve was estimated as the percentage of the total cross-area of plasmodesmata (including the cell membrane of the cytoplasmic sleeve).

Samples were collected in six independent experiments. Altogether, 15–20 bundles were analysed per line per experimental variant. Sets of three or four vascular bundles on separate sections were obtained from separate leaves, which resulted in a high randomization of the data set. A total of 100–400 plasmodesmata were thus analysed at the KMS/BS interface, per treatment. Up to 60 plasmodesmata were analysed at BS/BS, BS/VP and VP/VP cell interfaces, per treatment. Only plasmodesmata of undisturbed shape were taken into account, thus decreasing the total number of plasmodesmata analysed by about 25 %. Data for KMS/BS

plasmodesmata were statistically analysed by chi-square test ( $P < 0.01$ , SAS, FREQ procedure).

3D-ultrastructure of plasmodesmata, was evaluated by electron tomography on selected leaf samples, using a JEM 1400 (Jeol Co.) at 80 kV with a tilt-rotate tomographic holder and a high resolution digital camera (CCD MORADA; Olympus Soft Imaging Solutions, Germany). For every selected sample, images were taken at 60 000 magnification from 60° to –60°, in steps of 1°. Each series (120 images) with defined common axis of rotation was exported in TIFF (multi page) and AVI format (available on request) using TEM software (Olympus Soft Imaging Solutions). From such series, several electron tomography micrographs taken every 15° were selected. Thus the three dimensional shape of plasmodesmata was determined showing the plasmodesmata membrane, desmotubule and internal sphincter using 3D CAD software (Pro/ENGINEER Software, Wf2; Parametric Technology Corporation, USA).

#### Immunogold localization of calreticulin and callose

For calreticulin, samples were harvested from plants chilled for 4 h. Control (unchilled) plants were taken after 4 h of exposure to light. The location of calreticulin was determined immunologically (Baluška *et al.*, 1999) using polyclonal calreticulin antibody (gift from Dr F. Baluška) diluted 1 : 20 and goat anti-rabbit secondary antibody conjugated to 10-nm gold particles.

For callose, samples were harvested from plants chilled for 4 and 28 h. Control (unchilled) plants were taken after 4 of exposure to light. Immunolocalization of callose was performed following the method of Ferguson *et al.* (1998) using a monoclonal callose antibody (Biosupplies, Australia) diluted 1 : 100 and goat anti-mouse secondary antibody conjugated to 10-nm gold particles.

Material for immunocytolocalization of both calreticulin and callose was collected in three experiments. In the case of callose, gold particles were counted per plasmodesmata (out of approx. 100 PD). Data were statistically analysed by the permutation test ( $P < 0.01$ , SAS, NPAR1WAY procedure). The permutation test (also called exact or randomization test) is nonparametric, and makes no assumption regarding statistical distribution. It can be used for categorical, ordinal and metric data. This method is based on reference distribution, constructed by calculating all values of the test statistic for permutations of data (random assignment to treatment groups). From this distribution  $P$ -values are computed.

## RESULTS

#### Photosynthesis and transport kinetics

Maximal quantum yield of PS II electron transport ( $F_v/F_m$ , ratio of variable to maximal fluorescence) showed higher photoinhibition in chilled leaves of the chilling-sensitive CM 109 (CS) line (Table 1) compared with the chilling-tolerant KW 1074 (CT) line. Also, photosynthesis and transport parameters were inhibited by low temperature more strongly in the CS than in the CT line (Table 2). When measured at 14 °C, the largest difference was in the time of  $^{14}\text{C}$ -assimilate appearance in the transport path (AT), which increased much more in the CS (approx. 120 %) than in the

TABLE 1. Maximal quantum yield of PSII electron transport ( $F_v/F_m$ ; mean  $\pm$  s.d.) in leaves of two maize inbred lines treated with low temperature ( $14^\circ\text{C}$ ) for different time periods

	KW 1074	CM 109
Growth at $24^\circ\text{C}$	$0.748 \pm 0.021^a$	$0.756 \pm 0.011^a$
Chilling for 4 h	$0.729 \pm 0.018^a$	$0.715 \pm 0.010^b$
Chilling for 28 h	$0.697 \pm 0.021^b$	$0.647 \pm 0.032^c$

Measurements were done at  $24^\circ\text{C}$ . Data represent means for nine plants. Significant differences ( $P < 0.05$ ) within columns, estimated by analysis of variance, are indicated by different letters.

CT (approx. 60%) line (Table 2, cols III and IV, row 2). Measurements at  $24^\circ\text{C}$  on plants chilled for a short time (1 h, 4 h) demonstrated that changes in Pn, AT and RL were almost fully reversible in CT but irreversible in CS after just 1 h of chilling (Table 2, rows 1, 3 and 4).

Prolonged chilling at  $14^\circ\text{C}/12^\circ\text{C}$  (day/night) led to further changes in the transport parameters in the CS line, measured at both  $24^\circ\text{C}$  and  $14^\circ\text{C}$  (Table 2, cols IV and VI, rows 5 and 6). In the CT line similar changes were observed (Table 2, cols III and V, rows 5 and 6), but expressed much less than in CS.

#### Plasmodesmata ultrastructure

The ultrastructure of plasmodesmata-linking cells of vascular bundles, bundle sheath and Kranz mesophyll in control leaves was typical for maize (Evert *et al.*, 1977). The plasmodesmata that traversed the walls between KMS and BS had an internal electron-dense ring inside a cavity at the mesophyll side (Fig. 2A, E). This ring, called an 'internal sphincter' (Evert *et al.*, 1977), was composed of globular element, as deduced from the 3D structure of the KMS/BS plasmodesma from tomography (Fig. 2E). The cytoplasmic sleeve was constricted mostly in the middle region. The plasmodesmata at BS/BS, BS/VP and VP/VP interfaces were simple, only rarely branched, channels with the cytoplasmic sleeve slightly or not constricted at both neck regions and in the middle lamella region (Fig. 2C, G).

Chilling led to a strong swelling of sphincters in some plasmodesmata between KMS and BS cells in the CS line (Fig. 2B and F). Just after 1 h of chilling, about 17% of the plasmodesmata demonstrated enlargement of the sphincters and after 4 h of chilling the fraction of sealed plasmodesmata increased to about 30% (Table 3). Simultaneously, in the CT line, sphincters were enlarged only in 3–6% of the KMS/BS plasmodesmata (Table 3).

In the CS line, chilling led also to the constriction of cytoplasmic sleeves of plasmodesmata crossing the BS/VP cell interfaces (Figs 2D, H and 3A) as well as BS/BS and VP/VP interfaces (Fig. 3B, C). The constriction of the cytoplasmic sleeve was visible along the entire plasmodesma, mostly in the neck regions. Expressed as the percentage of the cross-area of the whole plasmodesmata, the cross-area of the cytoplasmic sleeve decreased from about 54% in control plants to about 45% after 1 h of chilling and to 35% on the second day of chilling. The cross-area of the cytoplasmic sleeve of plasmodesmata at BS/BS and VP/VP interfaces decreased from about 53% in control plants to about 43% after 1 h of chilling and did not change further with the duration of the chilling (Fig. 3B, C). In contrast to the CS line, in the CT line the low temperature did not cause any change to the mentioned plasmodesmata (Fig. 3).

#### Immunogold localization of calreticulin and callose

Control plants, as well as plants chilled for 4 h, showed a little callose at the cell wall, generally close to plasmodesmata (Figs 4G, H and 5G, H). There were no differences between lines in callose distribution either observed directly on slides (Figs 4 and 5) or by counting the gold particles (Table 4). However, after 28 h of chilling-treatment, callose over-accumulated strongly around KMS/BS and particularly BS/VP plasmodesmata in CS, but not in CT (Figs 4 and 5). To evaluate statistical differences between maize lines in respect to callose over-accumulation near plasmodesmata, gold particles were counted and the differences were estimated by a non-parametric, permutation test (see Materials and methods). It confirmed that the over-accumulation of callose around KMS/BS and particularly BS/VP in CS line after 28 h of chilling was statistically significant (Table 4).

TABLE 2. Net  $\text{CO}_2$  assimilation rate and transport parameters in seedlings of two maize inbred lines treated with low temperature ( $14^\circ\text{C}$ ) for different time periods

row/column	Treatment	Net $\text{CO}_2$ assimilation rate ( $\mu\text{mol CO}_2 \text{ m}^{-2} \text{ s}^{-1}$ )		Time taken for $^{14}\text{C}$ -photosynthates to appear in the transport path, AT (min)		Radioactivity exported from leaves, RL (% of total radioactivity incorporated)	
		KW 1074	CM 109	KW 1074	CM 109	KW 1074	CM 109
		I	II	III	IV	V	VI
1	Growth at $24^\circ\text{C}$ , measurement at $24^\circ\text{C}$	$16.1 \pm 1.4^a$	$17.8 \pm 2.1^a$	$5.8 \pm 1.2^a$	$6.9 \pm 0.6^a$	$56.3 \pm 6.1^a$	$55.0 \pm 8.8^a$
2	Growth at $24^\circ\text{C}$ , measurement at $14^\circ\text{C}$	$11.9 \pm 1.5^b$	$10.8 \pm 1.6^b$	$9.3 \pm 1.1^b$	$15.0 \pm 1.2^c$	$44.3 \pm 4.0^b$	$37.1 \pm 4.6^b$
3	Chilling for 1 h, measurement at $24^\circ\text{C}$	$16.1 \pm 3.0^a$	$12.3 \pm 1.8^b$	$5.8 \pm 0.7^a$	$7.9 \pm 1.3^{ab}$	$63.8 \pm 13.2^a$	$44.1 \pm 5.6^b$
4	Chilling for 4 h, measurement at $24^\circ\text{C}$	$15.0 \pm 1.3^a$	$11.4 \pm 0.5^b$	$5.0 \pm 0.9^a$	$9.8 \pm 0.5^b$	$61.0 \pm 7.5^a$	$38.3 \pm 4.1^b$
5	Chilling for 28 h, measurement at $24^\circ\text{C}$	$14.3 \pm 0.8^a$	$12.6 \pm 1.9^b$	$7.1 \pm 0.6^a$	$10.8 \pm 0.8^b$	$47.4 \pm 4.1^b$	$35.0 \pm 5.5^b$
6	Chilling for 28 h, measurement at $14^\circ\text{C}$	$9.6 \pm 2.9^b$	$8.7 \pm 1.3^b$	$9.9 \pm 0.6^b$	$17.8 \pm 1.2^c$	$36.3 \pm 4.8^c$	$16.0 \pm 3.1^c$

Data represent means  $\pm$  s.d. for 9–12 plants.

Significant differences ( $P < 0.05$ ) within columns, estimated by analysis of variance, are indicated by different letters.

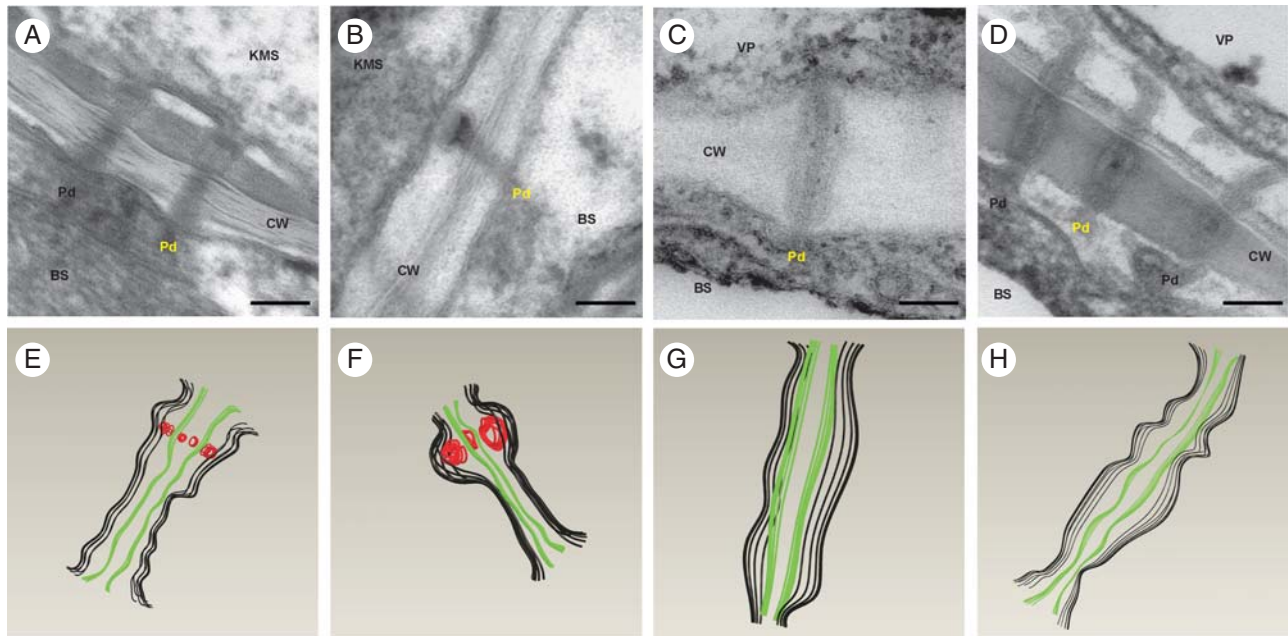


FIG. 2. Longitudinal sections of plasmodesmata in control and chilled leaves of the CM 109 maize inbred line: (A–D) electron micrograms; (E–H) corresponding 3D shapes, designed with 3D CAD software, of the plasmodesmata shown in the micrograms in (A) to (D) (see Materials and methods), in which black lines = cytoplasmic sleeves, green lines = desmotubules and red lines = internal sphincters. (A, E) KMS/BS plasmodesmata in control leaves, showing an electron-dense ring consisting of regular elements (internal sphincter) at the KMS side. (B, F) KMS/BS cell plasmodesmata in chilled leaves of CM 109 line, showing a strongly enlarged internal sphincter. (C, G) BS/VP plasmodesmata in control leaves. (D, H) BS/VP plasmodesmata in chilled leaves – strong constriction, particularly at neck regions. KMS, Kranz mesophyll; BS, bundle sheath; VP, vascular parenchyma; CW, cell wall; ER, endoplasmic reticulum; Pd, plasmodesmata. Scale bar = 100 nm.

In both lines, control plants showed no regular pattern of distribution of calreticulin in cells, despite its localization in the ER (Fig. 6B, D, F, G), or in the CT line after 4 h at sub-optimal temperature (Fig. 6C, E). In the CS line, however, strong immunolabelling of calreticulin occurred in the neck regions of plasmodesmata, on the BS side crossing the KMS/BS and BS/VP interfaces after chilling for 4 h (Fig. 6H, I). No immunogold labelling was found when the primary antibody was omitted in the immunolabelling procedure (Fig. 6A).

## DISCUSSION

In this work, the effects of chilling in two maize inbred lines, chilling-tolerant KW 1074 (CT) and chilling-sensitive CM 109 (CS) were analysed by measuring the rate of photosynthesis and photosynthate transport kinetics, the ultrastructure of plasmodesmata linking the KMS, BS and VP cells, and the mechanism of the closure of these plasmodesmata at low temperature.

### Leaf physiology

The physiological reactions (maximal efficiency of PSII, photosynthesis, photosynthate export) of seedlings to chilling (14 °C) were much greater in the CS line than in the CT line (Tables 1 and 2). Chilling sensitivity of maize is very often attributed to the susceptibility of photosynthesis, related to photoinhibition of PSII, enzyme inhibition, insufficient activity of anti-oxidant systems, etc. (Foyer *et al.*, 2002). However, the inbred lines in this study do not differ distinctly in photosynthetic enzyme activities or carotenoid composition

and amounts when grown at optimal temperature (Picatto, 1992; Haldimann, 1998). This suggests that inhibition of photosynthesis at low temperature is due to other mechanisms, particularly to inhibition of photosynthate export.

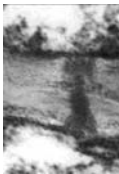
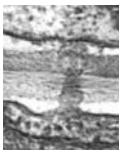

Support for such a hypothesis comes from the transport kinetics. It is particularly interesting that, upon chilling, there was a more than 2-fold increase in the time necessary for photosynthates to appear in the transport path in CS (Table 2, col. IV, row 2), suggesting a strong delay of sucrose transfer into the phloem loading zone in that line. It should be emphasized that a strong delay of photosynthate transfer into the transport path is the general feature of all chilling-sensitive maize dent inbred lines studied (Sowiński, 1995), thus providing the rationale for studying this phenomenon more thoroughly.

Even after very short chilling, the inhibition of photosynthesis, photosynthate transfer into the transport path and photosynthate export from leaves are irreversible and do not return to normal values after re-warming in the CS line. Since the photosynthate transport from KMS to VP cells takes the symplasmic route, ultrastructural changes of plasmodesmata linking Kranz mesophyll cells and bundle sheath cells, where C<sub>4</sub> photosynthesis takes place, as well as plasmodesmata linking bundle sheath and vascular parenchyma cells, were measured since that interface is important for sucrose export (Botha *et al.*, 2000).

### Changes in plasmodesmata ultrastructure

In the CS line, in contrast to CT, low temperature-induced swelling of the sphincters of plasmodesmata linking KMS and BS cells (Fig. 2 and Table 3) and decreased the lumen

TABLE 3. Number of plasmodesmata showing swelling of sphincter among plasmodesmata at mesophyll/bundle sheath interfaces in seedlings of two maize inbred lines chilled (14 °C) for different time periods

	KW 1074										CM 109										Example
	Control		1 h		4 h		12 h		28 h		C		1 h		4 h		12 h		28 h		
Total examined:	137		175		162		311		142		153		386		315		186		133		
Not defined	Mean	% of total	Mean	% of total	Mean	% of total	Mean	% of total	Mean	% of total	Mean	% of total	Mean	% of total	Mean	% of total	Mean	% of total	Mean	% of total	
	30	21.9	70	40.0	24	14.8	82	26.4	34	23.9	45	29.4	127	32.9	118	37.5	40	21.5	40	30.1	
Therefore total analysed	107		105		138		229		108		108		259		197		146		93		
Opened	107		100		130		221		105		108		216		140		109		71		
Closed	Mean	% of total analysed	Mean	% of total analysed	Mean	% of total analysed	Mean	% of total analysed	Mean	% of total analysed	Mean	% of total analysed	Mean	% of total analysed	Mean	% of total analysed	Mean	% of total analysed	Mean	% of total analysed	
	0	0	5	4.8	8	5.8	8	3.5	3	2.8	0	0	43*	16.6	57*	28.9	37*	25.3	22*	23.7	

1 h, 4 h, 12 h, 28 h, time of chilling; see Materials and methods.  
Data were collected in six independent experiments.

\* Significant differences ( $P < 0.05$ ) estimated by chi-square test.

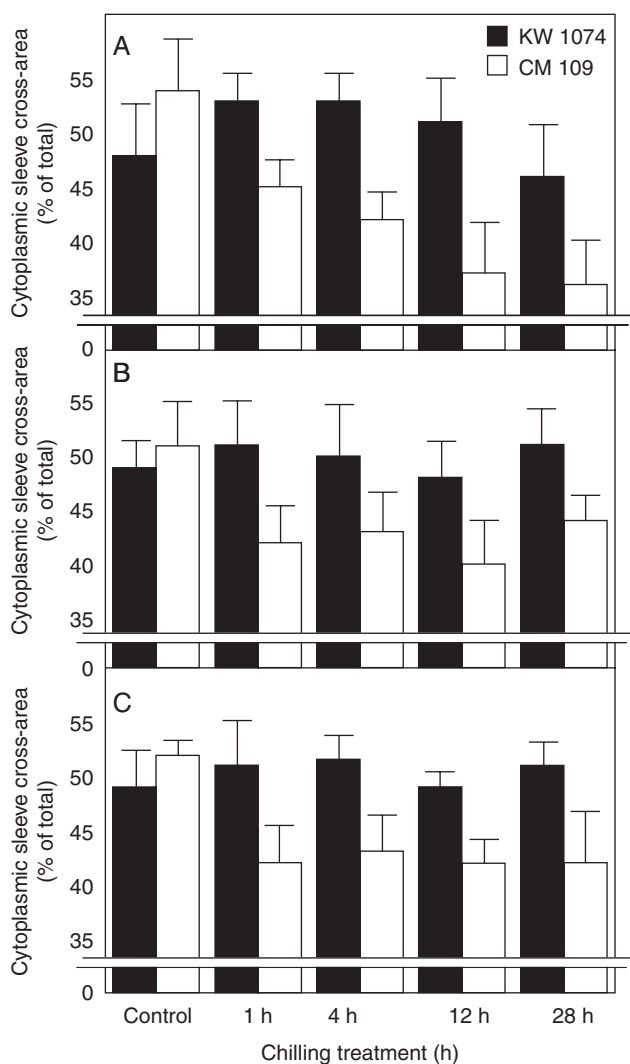


FIG. 3. Cross-area of cytoplasmic sleeve of plasmodesmata in control and chilled (1 h, 4 h, 12 h, 28 h) leaves of two maize inbred lines: (A) plasmodesmata at bundle sheath–vascular parenchyma (BS/VP) interface; (B) plasmodesmata at bundle sheath–bundle sheath (BS/BS) interface; (C) plasmodesmata at vascular parenchyma–vascular parenchyma (VP/VP) interface. KW 1074, chilling-tolerant line and CM 109, chilling-sensitive line, as indicated. Values are percentages of whole cross-area of plasmodesmata, including plasmalemma. Values are means of 40–50 plasmodesmata  $\pm$  s.e.

of the cytoplasmic sleeve of plasmodesmata between the BS and VP cells (Figs 2 and 3). The question arises, however, if the constriction of plasmodesmata observed under electron microscope reflected the real plasmodesmata behaviour in the leaf. Plasmodesmata are small and delicate structures, which could be modified during chemical fixation. A rapid plasmodesmata constriction was found, however, in another study (Schulz, 1995) where samples were also fixed by a standard method. Also, Botha *et al.* (1993) demonstrated that images of plasmodesmata fixed chemically were representative of their real structure. Additionally, one should note that leaves of both lines used in this study (control and chilling-treated) were fixed in exactly the same manner; therefore, the observed different pattern of plasmodesmata ultrastructure changes must reflect the different status of the plasmodesmata in the two

lines. Thus, following Waigmann and Zambrzycki (2000), it is concluded that constricted plasmodesmata, found in the CS line, do indeed represent ‘closed’ plasmodesmata.

The chilling-induced swelling of the electron-opaque structures at the mesophyll side of plasmodesmata linking Kranz mesophyll cells and bundle sheath cells found in the CS line is particularly difficult to interpret. The nature of the elements forming the sphincter in KMS/BS plasmodesmata is a matter of speculation. According to Olesen (1979), tannic acid used in the fixative (as in the present work) protects protein components from dehydration during fixation. Therefore, enlarged electron-dense elements at mesophyll side of KMS/BS plasmodesmata found in the CS line at low temperature possibly reflect real structures. Similarly, in deactivated apical meristems of *Betula pubescens*, sphincters fixed with the addition of tannic acid were much enlarged (Rinne and van der Schoot, 1998). It has been suggested that the neck region of the plasmodesma might be regulated by centrin attached to anchoring proteins (Overall and Blackmann, 1996). It should be noted, however, that such a model was postulated for extracellular sphincters (e.g. as in *Betula pubescens*), while the electron-dense structures in neck regions of plasmodesmata linking KMS and BS cells in maize (Evert *et al.*, 1977), sugarcane leaves (Robinson-Beers and Evert, 1991) and some other monocots (Botha *et al.*, 2007) are apparently located inside the cytoplasmic sleeve. Therefore the term sphincter, as proposed by Evert *et al.* (1977), may be questioned in the case of these structures. Despite the terminology, enlargement of electron-dense structures at the mesophyll side of KMS/BS plasmodesmata found in the CS line at low temperature show that even the moderate chilling often experienced by maize in a temperate climate, affects the ultrastructure of the KMS/BS plasmodesmata. However, the sealing mechanism in these plasmodesmata might be different from that in the extracellular sphincters.

#### Leaf physiology versus plasmodesmata closure

It is apparent that the slower export of  $^{14}\text{C}$ -assimilate to the phloem (AT) in CS fits very well with the observed ultrastructural changes of plasmodesmata linking the cells on the way from mesophyll to vascular parenchyma. This is supported by the fact that after a short period of chilling, the transport parameters and photosynthetic, even when measured at 24 °C did not recover to the control values in the CS line (Table 2, cols II, IV and VI, rows 3 and 4), where the closure of plasmodesmata at KMS/BS/VP interfaces was observed (Figs 2 and 3 and Table 3), particularly in the neck regions. In contrast to the CS line, the changes in the transport and photosynthesis upon chilling were reversible in the CT line (Table 2, cols I, III and V, rows 3 and 4), also showing no constriction of plasmodesmata. Theoretical considerations have led Anisimov and Egorov (2002) to propose that neck-region constriction or relaxation should determine the flow of solutes through the cytoplasmic sleeve. Also, Botha *et al.* (2007) consider that internal sphincters or collars could be responsible for controlling flow rates through the suberin-encased walls, such KMS/BS cell walls. Thus, it is reasonable to assume that constriction of leaf plasmodesmata in the CS line inhibits the flow of photosynthates between KMS and BS as well as from BS to VP cells, and this, in turn,

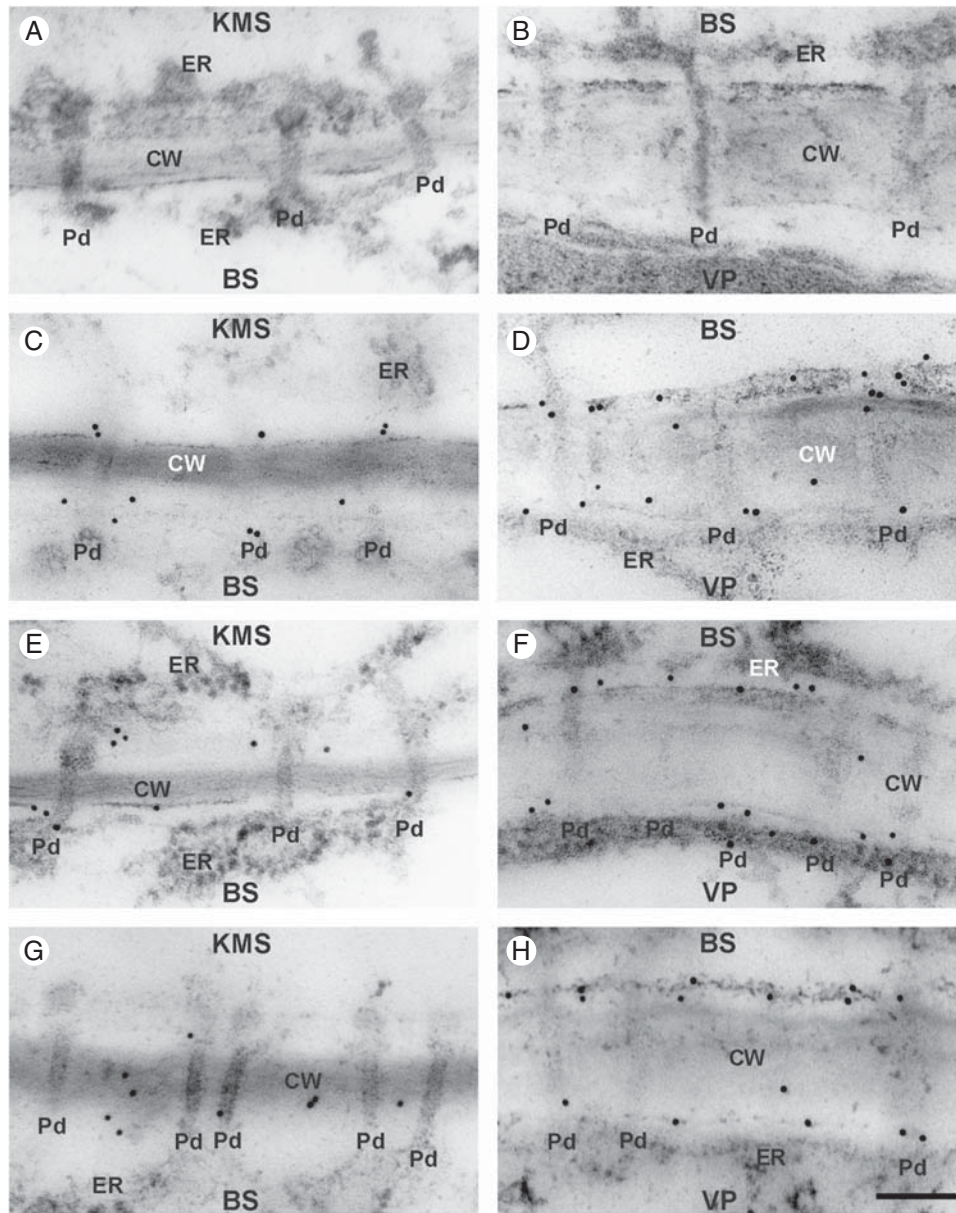


FIG. 4. Immunogold localization of callose in control and chilled (4 h, 28 h) leaves of the KW 1074 maize inbred line (CT): (A, B) negative control – no immunogold labelling when primary antibody was omitted; (C, E, G) KMS/BS interface; (D, F, H) BS/VP interface. Note some callose labelling in the cell wall close to the plasmodesma in control leaves (C, D) and those chilled for 4 h (E, F) and 28 h (G, H). Abbreviations: CT, chilling-tolerant line; KMS, Kranz mesophyll; BS, bundle sheath; VP, vascular parenchyma; CW, cell wall; ER, endoplasmic reticulum; Pd, plasmodesmata. Scale bar = 100 nm.

leads to the inhibition of photosynthesis. The feedback regulation of photosynthesis by accumulation of photosynthates is discussed in many reviews (e.g. Paul and Foyer, 2001). In maize, chilling-inhibition of transport of key photosynthetic intermediates, 3-phosphoglycerate, triose phosphate and some antioxidants between KMS and BS cells may have an adverse effect on function and survival (Foyer *et al.*, 2002).

In addition to the plasmodesmata at KMS/BS and BS/VP interfaces, plasmodesmata linking the VP cells and thick-walled sieve tubes may also have impact on the export of photosynthates from leaves. According to Fritz *et al.* (1983), thick-walled sieve tubes, which are not involved in long-distance transport, may take current photosynthates from VP cells and

transfer them to thin-walled sieve tubes. No apparent changes in ultrastructure of plasmodesmata linking VP cells and thin-walled sieve tubes were observed in chilling-treated maize leaves (data not shown). Also, no expression of calreticulin and over-accumulation of callose were observed near plasmodesmata of that type in chilled leaves. Thus, chilling may have minor effect on loading of photosynthates to the thick-walled sieve tube by a symplasmic route in juvenile maize leaves.

#### *The mechanism of plasmodesmatal closure at low temperature*

Plasmodesmatal closure under abiotic stress has been discussed in the literature as the effect of callose accumulation



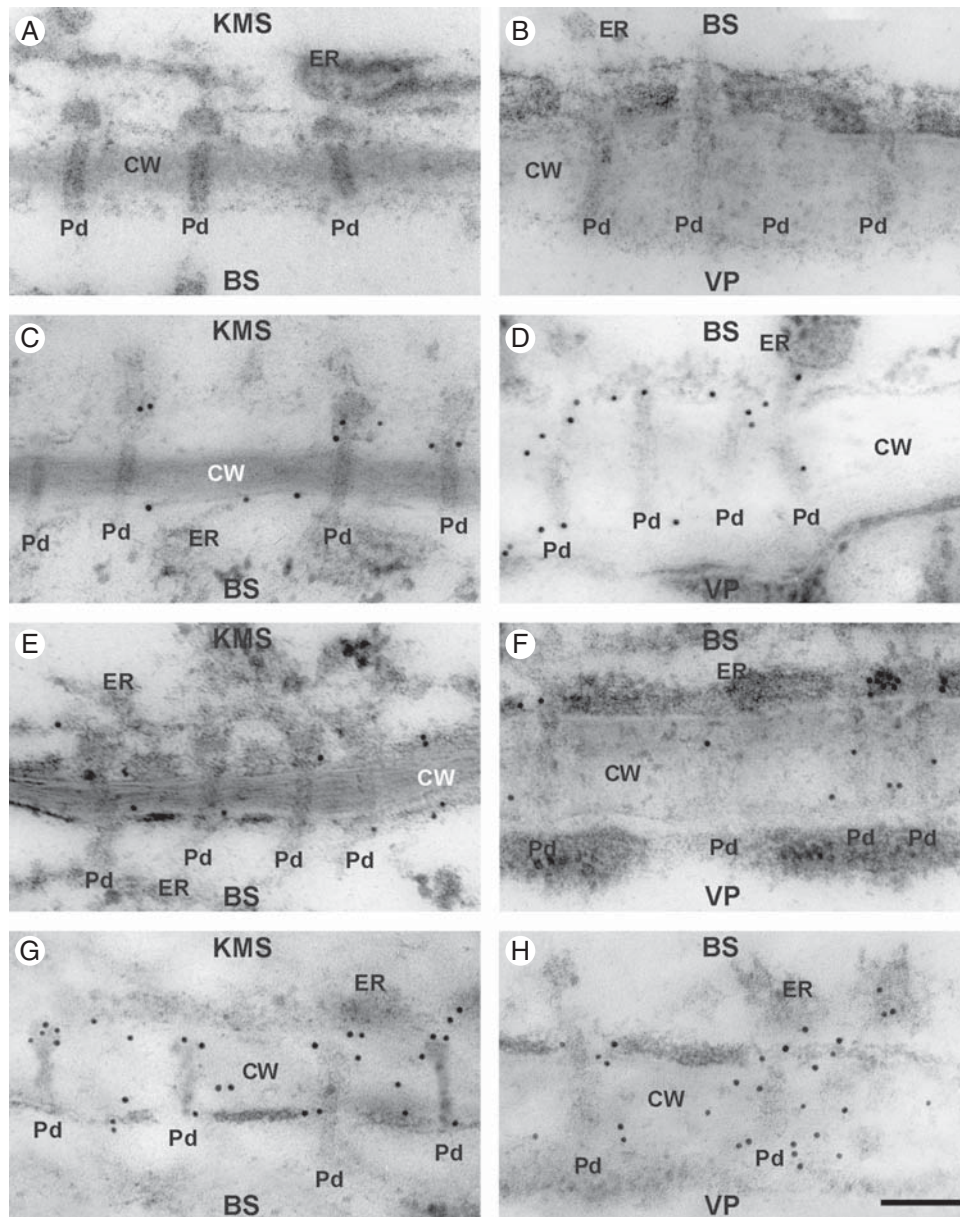


FIG. 5. Immunogold localization of callose in control and chilled (4 h, 28 h) leaves of the CM 109 maize inbred line (CS): (A, B) negative control; no immunogold labelling when primary antibody was omitted; (C, E, G) KMS/BS interface; (D, F and H) BS/VP interface. Note some callose labelling in cell wall close to the plasmodesma region in control leaves (C, D) and those chilled for 4 h (E, F). Note strong callose labelling near the plasmodesmata in leaves chilled for 28 h (G, H). Abbreviations: CS, chilling-sensitive line; KMS, Kranz mesophyll; BS, bundle sheath; VP, vascular parenchyma; CW, cell wall; ER, endoplasmic reticulum; Pd, plasmodesmata. Scale bar = 100 nm.

TABLE 4. The number of gold particles (mean  $\pm$  s.d.) conjugated to goat anti-rabbit secondary antibody-monoclonal 1  $\rightarrow$  3  $\beta$ -D-glucan antibody-callose at plasmodesmata region in leaf cells in two maize inbred lines treated with low temperature for different time periods

	KW 1074		CM 109	
	KMS/BS	BS/VP	KMS/BS	BS/VP
Growth at 24 °C	1.72 $\pm$ 0.51 <sup>a</sup>	3.29 $\pm$ 0.93a	2.05 $\pm$ 0.84 <sup>a</sup>	3.16 $\pm$ 2.07 <sup>a</sup>
Chilling for 4 h	2.02 $\pm$ 1.19 <sup>a</sup>	3.61 $\pm$ 1.61 <sup>a</sup>	2.07 $\pm$ 1.04 <sup>a</sup>	3.17 $\pm$ 1.23 <sup>a</sup>
Chilling for 28 h	1.75 $\pm$ 0.85 <sup>a</sup>	3.65 $\pm$ 0.51 <sup>a</sup>	3.02 $\pm$ 1.1 <sup>b</sup>	5.44 $\pm$ 1.51 <sup>b</sup>

Data were collected in three independent experiments. Each variant was estimated on the basis of at least ten vascular bundles. Significant differences ( $P < 0.01$ ) within columns, estimated by permutative test are indicated by different letters.

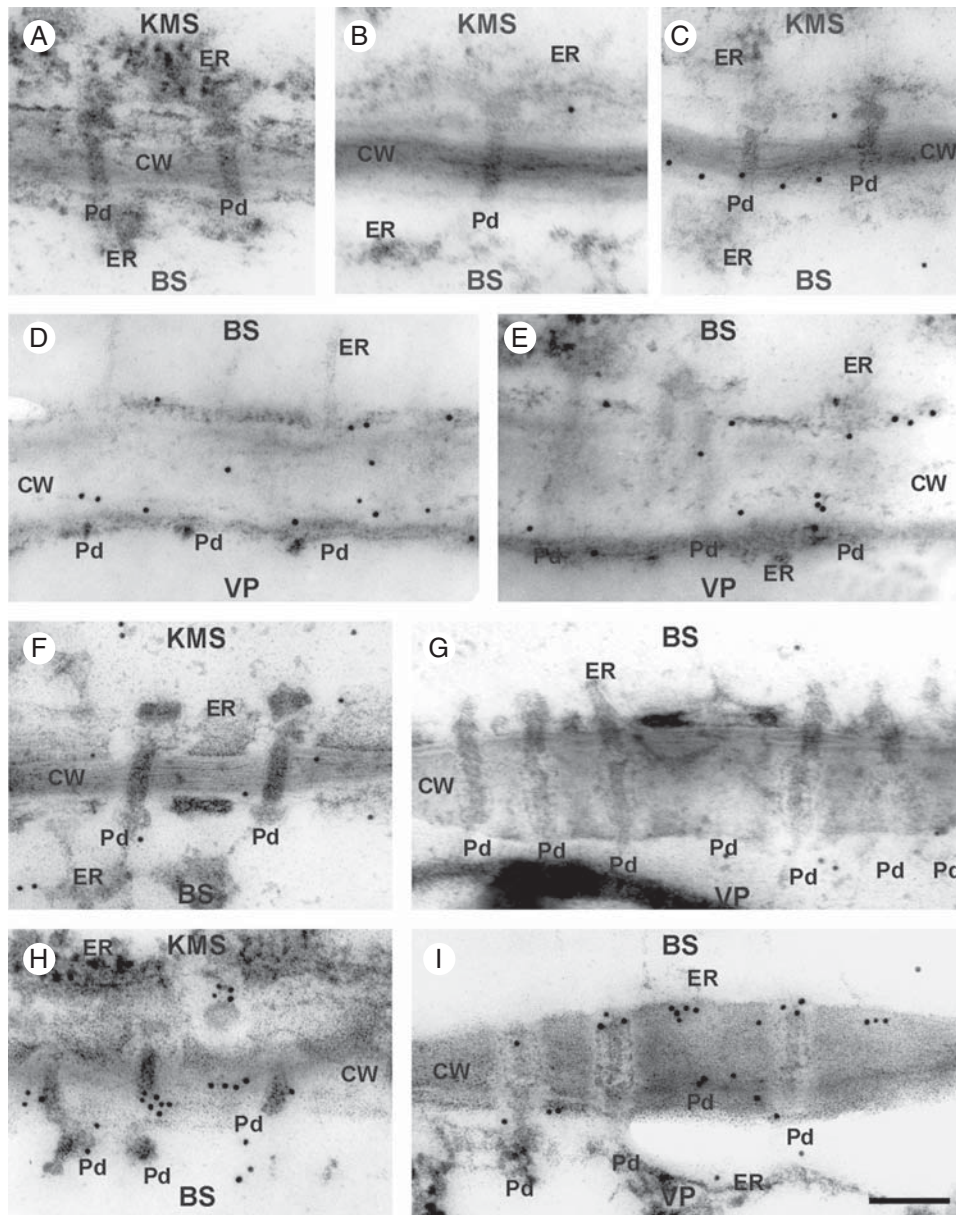


FIG. 6. Immunogold localization of calreticulin in control and chilled (4 h) leaves of KW 1074 (CT) and CM 109 (CS) maize inbred lines: (A) negative control – no immunogold labelling when primary antibody was omitted; (B–E) CT line showing the KMS/BS (B, C) and BS/VP (D, E) interfaces in which calreticulin localizes mostly to ER and CW in both control (B, D) and chilled (C, E) leaves; (F–I) CS line showing KMS/BS (F) and BS/VP (G) interfaces in control leaves, in which calreticulin localizes mostly to ER and CW, and KMS/BS (H) and BS/VP (I) interfaces in chilled leaves, in which calreticulin accumulates at the neck regions of the plasmodesmata, mostly at the BS side. Abbreviations: CT, chilling-tolerant line; CS, chilling-sensitive line; KMS, Kranz mesophyll; BS, bundle sheath; VP, vascular parenchyma; CW, cell wall; ER, endoplasmic reticulum; Pd, plasmodesmata. Scale bar = 100 nm.

near the plasmodesmata (Drake *et al.*, 1978; Radford *et al.*, 1998; Botha and Cross, 2000; Sivaguru *et al.*, 2000; Ueki and Citovsky, 2005; Levy *et al.*, 2007). Immunogold cytolocalization of callose in maize did show over-accumulation in KMS/BS/VP cell wall regions close to the plasmodesmata, but surprisingly only after prolonged treatment (28 h). No callose over-accumulation at KMS/BS/VP plasmodesmata was found after a short chilling-treatment (Figs 4 and 5 and Table 4), while they were already closed (Figs 2 and 3 and Table 3). It led us to search for another mechanism for fast plasmodesmatal closure at low temperature.

According to Baluška *et al.* (1999), calreticulin, due to its calcium buffering activity, could participate in plasmodesmata gating via modulation of calcium concentrations. Calreticulin was earlier found to be strongly expressed near closed plasmodesmata in roots, in response to different stresses: during plasmolysis (Baluška *et al.*, 1999) and aluminium stress (Sivaguru *et al.*, 2000). A similar phenomenon was found in chilled maize leaves, where the closure of KMS/BS/VP plasmodesmata in the CS line at low temperature was apparently mediated by calreticulin, which accumulated near the neck region (Fig. 6). It seems, therefore, that

calreticulin might be a universal mediator of fast plasmodesmatal closure.

### Conclusions

Inhibition of assimilate export due to inhibition of phloem loading and short-distance transport is an important factor determining the greater sensitivity of the photosynthetic apparatus to low temperature in some maize varieties than in others. We propose that the difference in chilling sensitivity of KW 1074 (CT) and CM 109 (CS) maize lines, is due to primary differences in the mechanism of assimilate transport. Stronger chilling sensitivity of CM 109 as compared with KW 1074, shown by decreased photosynthetic efficiency and assimilate export from a leaf, is related to changes in the ultrastructure of leaf plasmodesmata at low temperature. The chain of reactions to chilling is likely to include calreticulin action resulting in rapid and efficient closure of the plasmodesmata at both KMS/BS and BS/VP interfaces. Callose deposition in a leaf was a secondary effect of chilling-treatment. This new information provides a mechanism for understanding the chilling-sensitivity of maize, and how the function of the plasmodesma is regulated in the whole plant.

### ACKNOWLEDGEMENTS

We thank Dr J. Fronk, University of Warsaw for critical reading of the manuscript, Dr F. Baluška, Bonn University for the calreticulin antibody, Dr J. Leipner, ETH, Zürich for the seeds, R. Bartosiewicz for help in electron tomography, and E. Jarochovska and M. Jończyk for assistance in statistical analysis. Special thanks to H. Kos for help with the 3D plasmodesmata models.

### LITERATURE CITED

- Anisimov AV, Egorov AG. 2002. Plasmodesmata as a modulator of osmotic water fluxes in plants. *Russian Journal of Plant Physiology* 49: 677–684.
- Aoki N, Hirose T, Takahashi S, Ono K, Ishimaru K, Ohsugi R. 1999. Molecular cloning and expression analysis of a gene for a sucrose transporter in maize (*Zea mays* L.). *Plant and Cell Physiology* 40: 1072–1078.
- Baluška F, Šamaj J, Napier R, Volkmann D. 1999. Maize calreticulin localizes preferentially to plasmodesmata in root apex. *The Plant Journal* 19: 481–488.
- Blackmann LM, Harper JDI, Overall RL. 1999. Localization of a centrin-like protein to higher plant plasmodesmata. *European Journal of Cell Biology* 78: 297–304.
- Botha CEJ, Cross RHM. 2000. Towards reconciliation of structure with function in plasmodesmata: who is gatekeeper? *Micron* 31: 713–721.
- Botha CEJ, Hartley BJ, Cross RHM. 1993. The ultrastructure and computer-enhanced digital image analysis of plasmodesmata at the Kranz mesophyll-bundle sheath interface of *Themeda triandra* var. *imberbis* (Retz) A. Camus in conventionally fixed leaf blades. *Annals of Botany* 72: 255–261.
- Botha CEJ, Cross RHM, van Bel AJE, Peter CI. 2000. Phloem loading in the sucrose-export-defective (SXD-1) mutant maize is limited by callose deposition at plasmodesmata in bundle sheath-vascular parenchyma interface. *Protoplasma* 214: 65–72.
- Botha CEJ, Cross RHM, Liu L. 2007. Comparative structures of specialised monocotyledonous leaf blade plasmodesmata. In: Oparka KJ. ed. *Plasmodesmata*. New Delhi, India: Blackwell Publishing, 73–89.
- Doulis AG, Debian N, Kingston-Smith AH, Foyer CH. 1997. Differential localization of antioxidants in maize leaves. *Plant Physiology* 114: 1031–1037.
- Drake GA, Carr DJ, Anderson WP. 1978. Plasmolysis, plasmodesmata and the electrical coupling of oat coleoptile cells. *Journal of Experimental Botany* 29: 1205–1214.
- Eastman PAK, Dengler NG, Peterson CA. 1988a. Suberized bundle sheaths in grasses (*Poaceae*) of different photosynthetic types. I. Anatomy, ultrastructure and histochemistry. *Protoplasma* 142: 92–111.
- Eastman PAK, Peterson CA, Dengler NG. 1988b. Suberized bundle sheaths in grasses (*Poaceae*) of different photosynthetic types. II. Apoplastic permeability. *Protoplasma* 142: 112–126.
- Evert RF, Eschrich W, Heyser W. 1977. Distribution and structure of the plasmodesmata in mesophyll and bundle sheath cells of *Zea mays* L. *Planta* 136: 77–89.
- Evert RF, Russin WA, Bosabaldis AM. 1996. Anatomical and ultrastructural changes associated with sink-to-source transition in developing maize leaves. *International Journal of Plant Science* 157: 247–261.
- Ferguson C, Teeri TT, Siilka-Aho M, Read SM, Bacic A. 1998. Location of cellulose and callose in pollen tubes and grains of *Nicotiana tabacum*. *Planta* 206: 452–460.
- Foyer CH, Vanacker H, Gomez LD, Harbinson J. 2002. Regulation of photosynthesis and antioxidant metabolism in maize leaves at optimal and chilling temperatures: review. *Plant Physiology and Biochemistry* 40: 659–668.
- Fritz E, Evert FR, Heyser W. 1983. Microautoradiographic studies of phloem loading and transport in the leaf of *Zea mays* L. *Planta* 159: 193–206.
- Furbank RT, Stitt M, Foyer CH. 1985. Intercellular compartmentation of sucrose synthesis in leaves of *Zea mays* L. *Planta* 164: 172–178.
- Gamalei YuV, van Bel AJE, Pakhomova MV, Sjutkina AV. 1994. Effects of temperature on the conformation of the endoplasmic reticulum and on starch accumulation in leaves with the symplasmic minor-vein configuration. *Planta* 194: 443–453.
- Greaves JA. 1996. Improving suboptimal temperature tolerance in maize: the search for variance. *Journal of Experimental Botany* 296: 307–323.
- Haldimann P. 1998. Low growth temperature-induced changes to pigment composition and photosynthesis in *Zea mays* genotypes differing in chilling sensitivity. *Plant, Cell & Environment* 21: 200–208.
- Holdaway-Clarke TL, Walker NA, Hepler PK, Overall RL. 2000. Physiological elevations in cytoplasmic free calcium by cold or ion injection result in transient closure of higher plant plasmodesmata. *Planta* 210: 329–335.
- Janda T, Szalai G, Ducruet J-M, Paldi E. 1998. Changes in photosynthesis in inbred maize lines with different degrees of chilling tolerance grown at optimum and suboptimum temperatures. *Photosynthetica* 35: 205–212.
- Levy A, Erlanger M, Rosenthal M, Epel BL. 2007. A plasmodesmata-associated  $\beta$ -1,3-glucanase in *Arabidopsis*. *The Plant Journal* 49: 669–682.
- Long SP. 1983. C<sub>4</sub> photosynthesis at low temperatures. *Plant, Cell & Environment* 6: 345–363.
- Olesen P. 1979. The neck constriction in plasmodesmata. *Planta* 144: 349–358.
- Overall RL, Blackmann LM. 1996. A model of the macromolecular structure of plasmodesmata. *Trends in Plant Sciences* 1: 307–311.
- Paul MJ, Foyer CH. 2001. Sink regulation of photosynthesis. *Journal of Experimental Botany* 52: 1383–1400.
- Picatto C. 1992. *Chilling effects on photosynthetic traits of maize genotypes*. PhD Thesis, ETH, Zürich, Switzerland.
- Provencher LM, Miao L, Sinha N, Lucas WJ. 2001. *Sucrose export defective1* encodes a novel protein implicated in chloroplast-to-nucleus signaling. *The Plant Cell* 13: 1127–1141.
- Radford JE, Vesk M, Overall RL. 1998. Callose deposition at plasmodesmata. *Protoplasma* 201: 30–37.
- Rinne PLV, van der Schoot C. 1998. Symplasmic fields in the tunica of the shoot apical meristem coordinate morphogenetic events. *Development* 125: 1477–1485.
- Robinson-Beers K, Evert RF. 1991. Fine structure of plasmodesmata in mature leaves of sugarcane. *Planta* 184: 307–318.
- Schulz A. 1995. Plasmodesmal widening accompanies the short-term increase in symplasmic phloem unloading in pea root tips under osmotic stress. *Protoplasma* 188: 22–37.
- Sivaguru M, Fujiwara T, Šamaj J et al. 2000. Aluminium induced 1  $\rightarrow$  3- $\beta$ -D-Glucan inhibits cell-to-cell trafficking of molecules through plasmodesmata: a new mechanism of aluminium toxicity in plants. *Plant Physiology* 124: 991–1005.
- Sowiński P. 1995. Transport of assimilates from leaves to roots in cold-treated maize seedlings: kinetics and assimilate distribution. *Acta Physiologia Plantarum* 17: 341–348.

- Sowiński P, Rudzińska-Langwald A, Kobus P. 2003.** Changes in plasmodesmata frequency in vascular bundles of maize seedling leaf induced by growth at suboptimal temperatures in relation to photosynthesis and assimilate export. *Environmental and Experimental Botany* **50**: 183–196.
- Thompson RG, Fensom DS, Anderson RR, Dronin R, Leiper W. 1979.** Translocation of  $^{14}\text{C}$  from leaves of *Helianthus*, *Heracleum*, *Nymphoides*, *Ipomoea*, *Tropaeolum*, *Zea*, *Fraxinus*, *Ulmus*, *Picea*, and *Pinus*: comparative shapes and some fine structure profiles. *Canadian Journal of Botany* **57**: 845–863.
- Ueki S, Citovsky V. 2005.** Identification of an interactor of cadmium ion-induced glycine-rich protein involved in regulation of callose levels in plant vasculature. *Proceedings of National Academy of Sciences, USA* **102**: 12089–12094.
- Verheul MJ, Picatto C, Stamp P. 1996.** Growth and development of maize (*Zea mays* L.) seedlings under chilling conditions in the field. *European Journal of Agronomy* **5**: 31–43.
- Waigmann E, Zambryski P. 2000.** Trichome plasmodesmata: a model system for cell-to-cell movement. *Advances in Botanical Research* **31**: 261–283.